


**Multipartite nonlocality in one-dimensional quantum chains: A transfer-matrix theory**Zhao-Yu Sun,<sup>1,\*</sup> Hui-Xin Wen,<sup>1</sup> Meng Li,<sup>1</sup> and Bin Guo<sup>2</sup><sup>1</sup>*School of Electrical and Electronic Engineering, Wuhan Polytechnic University, Wuhan 430023, China*<sup>2</sup>*Department of Physics, Wuhan University of Technology, Wuhan 430070, China* (Received 11 July 2021; revised 9 December 2021; accepted 11 January 2022; published 25 January 2022)

We propose a transfer-matrix theory to reveal the hidden structure in the multipartite nonlocality operators in one-dimensional (1D) quantum chains. The theory offers a unified description for the scaling behaviors of multipartite quantum nonlocality in general 1D quantum lattices. Furthermore, in order to figure out the hierarchy of multipartite nonlocality for infinite-size chains, powerful transfer-matrix-based algorithms are proposed. In quantum critical regions, the algorithms converge much faster than the traditional approach.

DOI: [10.1103/PhysRevA.105.012213](https://doi.org/10.1103/PhysRevA.105.012213)**I. INTRODUCTION**

For years entanglement entropy has been widely investigated in various low-dimensional quantum lattices [1]. The obtained knowledge in turn promotes the improvements of numerical simulation algorithms for these models [2]. It needs mention that entanglement entropy characterizes *bipartite* quantum entanglement. For typical quantum lattices which consist of many qubits, however, bipartite settings could not reveal all the features of entanglement in the models. Recently, quantum correlations with *multipartite* settings have attracted much attention, and the field is still in development [3–11].

A feasible approach to characterize multipartite quantum correlations is to use Bell-type inequalities [12–17]. For instance, Collins *et al.* show how to detect genuine  $n$ -partite correlations with Bell-type inequalities [12]. Several years later, the theory was generalized to a full family of multipartite correlations by Bancal *et al.* [15]. Moreover, nonlocality in systems with arbitrary dimensions [13,16] and networks [18,19] have also been discussed in several pioneering papers.

Multipartite correlations detected by Bell-type inequalities are called multipartite nonlocality. In the field of condensed matter physics, multipartite nonlocality has been used to characterize the ground states of various low-dimensional quantum lattices, including one-dimensional (1D)  $XY$  chains [20], transverse-field Ising chains [21,22],  $XXZ$  chains [23,24], ferromagnetic chains [25], two-leg spin ladders [26], two-dimensional (2D) transverse-field Ising lattices [27], Lipkin-Meshkov-Glick models [28], and many others [29]. It is found that multipartite nonlocality provides a valuable perspective for us to understand quantum phase transitions (QPTs) and critical phenomena [30] in these models.

In quantum lattice theory, scaling analysis is an important topic. It is found that multipartite nonlocality presents rich scaling behaviors in 1D quantum lattices. For instance, (i) in some parameter regions of the  $XY$  chains [20], the

nonlocality measure  $\mathcal{S}_n$  vanishes in the large- $n$  limit; (ii) in some other situations, such as the ferromagnetic states [20,26] and the antiferromagnetic states [24],  $\mathcal{S}_n$  turns out to be an  $n$ -independent nonzero constant, i.e.,  $\mathcal{S}_n \sim \text{const}$ ; (iii) nevertheless, in most situations (such as the critical transverse-field Ising chains [20,22,31],  $XXZ$  chains [24,31], and the two-leg spin ladders [26]),  $\mathcal{S}_n$  scales as  $\log_2 \mathcal{S}_n \sim \mathcal{K}n + b$ , with  $\mathcal{K}$  and  $b$  two fitting parameters. It is expected that an in-depth analysis about the *origin* of these scaling behaviors would greatly deepen our understanding of multipartite nonlocality in quantum chains. However, because of the complexity in the definition of multipartite nonlocality, as far as we know, the issue has not been discussed.

In this paper, a transfer-matrix theory will be proposed, which reveals the hidden translation invariance in the optimal nonlocality operators in 1D quantum chains. We will show that the scaling of  $\mathcal{S}_n$  is just determined by the largest-magnitude eigenvalue  $\lambda_{\max}$  of the transfer matrix in the model, i.e.,  $\mathcal{S}_n \sim |\lambda_{\max}|^n$ . It is quite clear that the above-mentioned three scaling behaviors correspond to situations with  $|\lambda_{\max}| < 1$ ,  $|\lambda_{\max}| = 1$ , and  $|\lambda_{\max}| > 1$ , respectively. Some further applications of the theory to improve numerical algorithms will also be discussed.

**II. BASIC CONCEPTS**

*Hierarchy of multipartite correlations and grouping numbers.* A key feature of multipartite correlations is that they can present various hierarchies (see Fig. 1). We consider a model consisting of six parties, i.e.,  $a_1, a_2, a_3, a_4, a_5$ , and  $a_6$ . One can always divide these parties into (at most)  $g$  groups such that only parties in the same group can share communications with each other. Then the grouping number  $g$  offers us an intuitive approach to characterize the hierarchy of multipartite correlations. In an extreme situation, every party cannot share any communication with other parties. Then we may label the model as  $\{\underline{a_1}, \underline{a_2}, \underline{a_3}, \underline{a_4}, \underline{a_5}, \underline{a_6}\}$  with a grouping number  $g = 6$  [Fig. 1(a)]. Suppose only parties  $a_1$  and  $a_2$  are allowed to share some communications with each other. Then the model can be labeled as  $\{\underline{a_1 a_2}, \underline{a_3}, \underline{a_4}, \underline{a_5}, \underline{a_6}\}$

\*Corresponding author: [sunzhaoyu2020@whpu.edu.cn](mailto:sunzhaoyu2020@whpu.edu.cn)

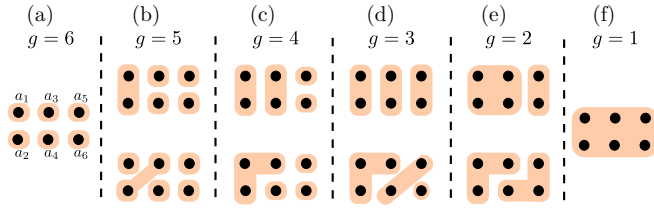


FIG. 1. Various patterns of multipartite quantum correlations in  $n$ -qubit quantum systems with  $n = 6$ . Qubits are denoted by black dots, and only qubits in the same shadow can share quantum correlations with each other. The leftmost one describes product states and the rightmost one describes genuine multipartite correlations. From left to right, the *hierarchy* of multipartite correlations increases gradually. The hierarchy can be captured by the nonlocality measure  $\mathcal{S}_n$  (for finite-size systems) and the central parameter  $\mathcal{K}$  (for infinite-size systems).

with a grouping number  $g = 5$  [Fig. 1(b)]. It is clear that models such as  $\{a_1, a_2a_3, a_4, a_5, a_6\}$  and  $\{a_1a_3, a_2, a_4, a_5, a_6\}$  also have a grouping number  $g = 5$ . Similarly, models such as  $\{a_1a_2, a_3a_4, a_5, a_6\}$  and  $\{a_1a_2a_3, a_4, a_5, a_6\}$  have a grouping number  $g = 4$  [Fig. 1(c)];  $\{a_1a_2, a_3a_4, a_5a_6\}$  and  $\{a_1a_2a_3, a_4a_5, a_6\}$  have a grouping number  $g = 3$  [Fig. 1(d)];  $\{a_1a_2a_3a_4, a_5a_6\}$  and  $\{a_1a_2a_3, a_4a_5a_6\}$  have a grouping number  $g = 2$  [Fig. 1(e)]; and  $\{a_1a_2a_3a_4a_5a_6\}$  have a grouping number  $g = 1$  [Fig. 1(f)].

It is quite clear that a smaller (larger) value of  $g$  indicates a higher (lower) hierarchy of multipartite correlations. For instance,  $g = n$  denotes product states and  $g = 1$  denotes the highest hierarchy of multipartite correlations (i.e., genuine  $n$ -partite correlations).

**Bell-type inequality and multipartite nonlocality.** For a quantum many-body state, the grouping number  $g$  can be analyzed numerically. First, one may design some subtle *expression*  $\mathcal{S}$  (an instance of  $\mathcal{S}$  will be introduced in the next section). Then one needs to figure out the maximal value  $\mathcal{S}_{g_0} = \max \mathcal{S}$  by considering *all* the models with a fixed grouping number  $g_0$ . Then for any model with a grouping number  $g_0$ , the following Bell-type inequality should hold, i.e.,  $\mathcal{S} \leq \mathcal{S}_{g_0}$ . For a concerned quantum state, one evaluates this inequality. If the inequality is violated, it becomes unambiguous that the multipartite correlations in the state cannot be reproduced by any  $g$ -grouping model. Thereby, one can conclude that the grouping number of the state should be (at most)  $g_0 - 1$ . In the literature, multipartite correlations observed by the violation of Bell-type inequalities are usually called multipartite nonlocality.

**Mermin-Klyshko-Bell inequalities.** A widely used expression for  $\mathcal{S}$  is proposed by Mermin and Klyshko [32–34]. First, we introduce the  $n$ -qubit nonlocality operator  $\hat{M}_n$ . On each qubit  $i$ , one should define two local observables as  $\hat{m}_i = \mathbf{a}_i \cdot \boldsymbol{\sigma}$  and  $\hat{m}'_i = \mathbf{a}'_i \cdot \boldsymbol{\sigma}$ , where  $\mathbf{a}_i$  and  $\mathbf{a}'_i$  are unit vectors and  $\boldsymbol{\sigma}$  are the Pauli matrices. Then the  $n$ -qubit nonlocality operator is defined recursively as

$$\begin{aligned} \hat{M}_n(\bar{\mathbf{a}}) &= \frac{1}{2} \hat{M}_{n-1} \otimes (\hat{m}_n + \hat{m}'_n) \\ &+ \frac{1}{2} \hat{M}'_{n-1} \otimes (\hat{m}_n - \hat{m}'_n), \end{aligned} \quad (1)$$

where  $\hat{M}'_{n-1}$  is obtained by exchanging all the  $\mathbf{a}_i$  and  $\mathbf{a}'_i$  in  $\hat{M}_{n-1}$ , and  $\bar{\mathbf{a}} = \{\mathbf{a}_1, \mathbf{a}'_1, \dots, \mathbf{a}_n, \mathbf{a}'_n\}$  is a set of  $2n$  unit vectors. In Eq. (1), a specific ordering ( $n, n-1, n-2, \dots, 1$ ) of the qubits has been used. Some discussions about other orderings can be found in the Appendix of this paper.

$\hat{M}_n$  is a member of the full-correlation nonlocality operators [34]. Compared with other nonlocality operators, a key advantage of  $\hat{M}_n$  is that [15] it provides explicit upper bounds for various *hierarchies* of multipartite correlations (Fig. 1).

For any  $n$ -qubit quantum state whose correlations can be reproduced by  $g_0$ -grouping models, it has been proved that the following Mermin-Klyshko-Bell inequality should hold [15]:

$$\mathcal{S}_n = \begin{cases} \max_{\bar{\mathbf{a}}} \langle \hat{M}_n(\bar{\mathbf{a}}) \rangle \leq 2^{\frac{n-g_0}{2}} & \text{for } n - g_0 \text{ is even} \\ \max_{\bar{\mathbf{a}}} \langle \hat{S}_n(\bar{\mathbf{a}}) \rangle \leq 2^{\frac{n-g_0}{2}} & \text{for } n - g_0 \text{ is odd,} \end{cases} \quad (2)$$

where the maximization is used to remove any dependence upon local measures,  $\langle \cdot \rangle$  denotes standard expectation value, and  $\hat{S}_n = \frac{1}{\sqrt{2}}(\hat{M}_n + \hat{M}'_n)$ . If the inequality is violated, one can conclude that the multipartite correlations in the state cannot be reproduced by any  $g$ -grouping model. In other words, the grouping number of the state should be (at most)  $g_0 - 1$ .

The index  $g_0$  with  $g_0 = 2, 3, \dots, n$  labels a complete set of Bell-type inequalities. The highest-rank one is  $\mathcal{S}_n \leq 2^{\frac{n-2}{2}}$  with  $g_0 = 2$ . If this Bell inequality is violated, the correlations in the state cannot be reproduced by any 2-grouping model. Thereby, the grouping number should be  $g = 1$ , i.e., genuine multipartite nonlocality [Fig. 1(f)]. The lowest-rank one is  $\mathcal{S}_n \leq 2^{\frac{n-n}{2}} = 1$  with  $g_0 = n$ . If it is violated, one concludes that the grouping number is (at most)  $n - 1$  [Fig. 1(b)]. Thereby, a *larger* (smaller)  $\mathcal{S}_n$  would indicate a *higher* (lower) hierarchy of multipartite nonlocality in the concerned  $n$ -qubit system.

As a highly nontrivial problem, the  $n$ -qubit numerical optimization with respect to  $\bar{\mathbf{a}}$  in Eq. (2) has been solved in Ref. [31]. It needs mention that the numerical optimal solutions, denoted as

$$\bar{\mathbf{a}}^* = \{\mathbf{a}_1^*, \mathbf{a}'_1^*, \dots, \mathbf{a}_n^*, \mathbf{a}'_n^*\}, \quad (3)$$

usually seem to be random numbers. Nevertheless, as we will show, tensor networks can clarify the origin of this randomness, and provide clues for us to understand the structure and the behavior of the optimal nonlocality operators. Moreover, in quantum lattices, one may be just interested in a qualitative description of multipartite correlations. Thereby, we ignore the parity in Eq. (2) and just consider  $\hat{M}_n(\bar{\mathbf{a}})$ .

### III. TRANSFER-MATRIX THEORY OF MULTIPARTITE NONLOCALITY

**Tensor network for  $\langle \hat{M}_n(\bar{\mathbf{a}}) \rangle$ .** The basis of our theory is the tensor network form of  $\langle \hat{M}_n(\bar{\mathbf{a}}) \rangle = \langle \psi | \hat{M}_n | \psi \rangle$ . First, it is well known that the ground states  $|\psi\rangle$  of 1D quantum chains can be described by matrix product states (MPSs) [2]. For instance, an infinite-size MPS consisting of one-qubit unit cells can be expressed as

$$|\psi\rangle = \sum_{\dots s_{-1} s_0 s_1 \dots} \text{tr}(\dots A_{s_{-1}} A_{s_0} A_{s_1} \dots) |\dots s_{-1} s_0 s_1 \dots\rangle, \quad (4)$$

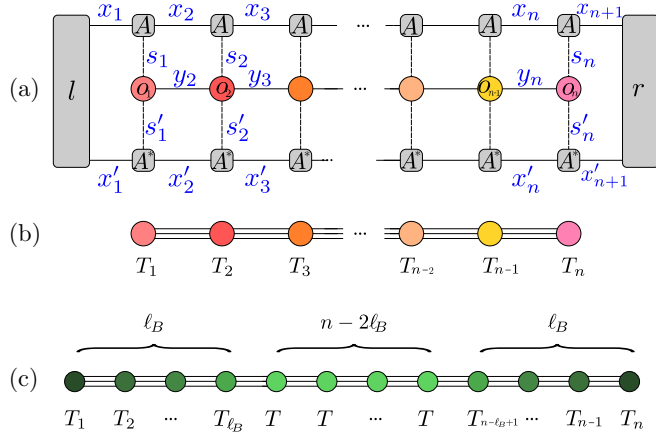


FIG. 2. (a) Tensor network for calculating  $n$ -qubit nonlocality measure  $\max_{\bar{a}} \langle \hat{M}_n(\bar{a}) \rangle$  in an infinite-size chain. As are translation-invariant tensors for the matrix product state  $|\psi\rangle$ , with  $l$  and  $r$  the environment tensors of the concerned subchain. Tensors  $o_i$  together form a tensor network for the nonlocality operator  $\hat{M}_n$ . (b) By tensor contractions on each qubit,  $\langle \hat{M}_n \rangle$  is further rephrased into a tensor train, i.e.,  $\langle \hat{M}_n \rangle = \langle T_1 | T_2 \cdots T_{n-1} | T_n \rangle$ . (c) To explain the general scaling of the nonlocality measure in 1D quantum chains, we propose a transfer matrix theory. That is, except for the boundary regions with depth  $\ell_B$ , by proper similarity transformations the optimal tensors  $T_i$  can be transformed into translation-invariant tensors, denoted by a transfer matrix  $T$ .  $\ell_B$  controls the accuracy of the transfer matrix theory, and when  $\ell_B \rightarrow \frac{n}{2}$ , (c) fully reproduces (b).

where  $s_i = 0, 1$  denote the local degree of freedom of the  $i$ th qubit, and  $A$  denotes a translation-invariant third-order tensor whose entry is  $A_{s_i x_i x_{i+1}}$  [see Fig. 2(a)]. Alternatively, one may treat  $A_{s_i}$  as  $D \times D$  matrices, with  $D$  the bond dimension of the MPS. When  $D$  is large enough, MPSs are able to describe the ground states of general 1D quantum chains faithfully.

In a quite recent paper [35], the  $n$ -qubit nonlocality operator  $\hat{M}_n(\bar{a})$  is also rephrased into a matrix product operator as  $\hat{M}_n(\bar{a}) = \langle o_1 | o_2 \cdots o_{n-1} | o_n \rangle$ , with

$$\langle o_1 | = (\hat{m}_1, \hat{m}'_1), \quad |o_n\rangle = \begin{pmatrix} \frac{1}{2}(\hat{m}_n + \hat{m}'_n) \\ \frac{1}{2}(\hat{m}_n - \hat{m}'_n) \end{pmatrix} \quad (5)$$

and

$$o_i = \begin{pmatrix} \frac{1}{2}(\hat{m}_i + \hat{m}'_i) & \frac{1}{2}(\hat{m}'_i - \hat{m}_i) \\ \frac{1}{2}(\hat{m}_i - \hat{m}'_i) & \frac{1}{2}(\hat{m}_i + \hat{m}'_i) \end{pmatrix} \text{ for } 1 < i < n. \quad (6)$$

The tensor network for  $\langle o_1 | o_2 \cdots o_{n-1} | o_n \rangle$  can be found in Fig. 2(a).  $\langle o_1 |$  is a third-order tensor whose entry can be expressed as  $(o_1)_{s_1 s'_1 y_2}$ . Similarly,  $|o_n\rangle$  is also a third-order tensor whose entry is  $(o_n)_{s_n s'_n y_n}$ . Moreover, for  $1 < i < n$ ,  $o_i$  is a fourth-order tensor whose entry is  $(o_i)_{s_i s'_i y_i y_{i+1}}$ . Alternatively, one can treat  $(o_1)_{s_1 s'_1}$  and  $(o_n)_{s_n s'_n}$  as vectors, and  $(o_i)_{s_i s'_i}$  as  $2 \times 2$  matrices when  $1 < i < n$ .

We are ready to deal with the expression  $\langle \hat{M}_n(\bar{a}) \rangle = \langle \psi | \hat{M}_n | \psi \rangle$ , which is defined on a continuous  $n$ -qubit subchain in the middle of an infinite-size MPS. It is not difficult to check that the left and right environment blocks of the subchain contain the products of many translation-invariant

matrices  $E$ , i.e.,  $\lim_{L \rightarrow \infty} E^L$ , with  $E$  given by [2]

$$E = \sum_{s_i} A_{s_i} \otimes A_{s_i}^*. \quad (7)$$

It is well known that  $\lim_{L \rightarrow \infty} E^L$  can be presented by the left and right eigenvectors  $\ell$  and  $r$  of the matrix  $E$ , corresponding to the largest eigenvalue.

Finally, combined with the expressions of  $|\psi\rangle$  and  $\hat{M}_n(\bar{a})$  and the simplified environment blocks, the average value  $\langle \hat{M}_n(\bar{a}) \rangle$  can be rephrased into a standard three-layer tensor network in Fig. 2(a).

To further simplify this tensor network, on each qubit  $i$  in the concerned subchain, we carry out local tensor contractions. First, for  $1 < i < n$ , we would define a local tensor  $T_i$  as

$$T_i(a_i, a'_i) = \sum_{s_i s'_i} A_{s_i} \otimes (o_i)_{s_i s'_i} \otimes A_{s'_i}^*. \quad (8)$$

Second, for the leftmost qubit, we take into account its left environment block  $\ell$ . Thereby a local tensor  $\langle T_1 |$  should be defined as

$$T_1(a_1, a'_1) = \sum_{s_1 s'_1} \ell A_{s_1} \otimes (o_1)_{s_1 s'_1} \otimes A_{s'_1}^*. \quad (9)$$

Similarly, for the rightmost qubit, a local tensor  $|T_n\rangle$  should be defined as

$$T_n(a_n, a'_n) = \sum_{s_n s'_n} A_{s_n} \otimes (o_n)_{s_n s'_n} \otimes A_{s'_n}^* r. \quad (10)$$

Finally, with these local tensors  $T_i$ , the three-layer tensor network of  $\langle \hat{M}_n(\bar{a}) \rangle$  in Fig. 2(a) is simplified into Fig. 2(b), i.e.,<sup>1</sup>

$$\langle \hat{M}_n(\bar{a}) \rangle = \langle T_1 | T_2 T_3 \cdots T_{n-2} T_{n-1} | T_n \rangle. \quad (11)$$

It is straightforward that the nonlocality measure  $\mathcal{S}_n$  [Eq. (2)] becomes

$$\mathcal{S}_n = \max_{\bar{a}} \langle \hat{M}_n(\bar{a}) \rangle = \max_{\bar{a}} \langle T_1 | T_2 T_3 \cdots T_{n-2} T_{n-1} | T_n \rangle. \quad (12)$$

*Origin of randomness in the optimal solutions.* In Eq. (12), it is quite clear that if some identity  $SS^{-1}$  is inserted into any two adjacent tensors  $T_i$  and  $T_{i+1}$ , the average value does not change. Consider two vector sets  $\bar{a}$  and  $\bar{b}$ , where the corresponding local tensors  $T_i(a_i, a'_i)$  and  $T_i(b_i, b'_i)$  are not equal to each other. It is possible that by some similarity transformations they can be transformed into each other. Consequently, it may turn out that  $\langle \hat{M}_n(\bar{a}) \rangle = \langle \hat{M}_n(\bar{b}) \rangle$  even if  $\bar{a} \neq \bar{b}$ . Two subsequent results are as follows. First, Eq. (12) has many optimal solutions  $\bar{a}^*$  which are equivalent to each other. Second, numerical optimization algorithms would converge *randomly* into one of these equivalent solutions, and thus the output solution  $\bar{a}^*$  would seem to be rather *random*. Consequently, it is difficult to disclose any hidden feature of the optimal nonlocality operator  $\hat{M}_n(\bar{a}^*)$  by analyzing the numerical solution  $\bar{a}^*$ .

<sup>1</sup>In Eqs. (8)–(10), the entries of these tensors are  $(T_i)_{x_i y_i x'_i y_{i+1} y_{i+1} x'_{i+1}}$ ,  $(T_1)_{1; x_2 y_2 x'_2}$ , and  $(T_n)_{x_n y_n x'_n; 1}$ , respectively. Thus, it is convenient to treat  $T_i$  as matrices,  $T_1$  as a bra vector, and  $T_n$  as a ket vector.

*Transfer matrix theory.* We call the tensors  $T_i = T_i(\mathbf{a}_i^*, \mathbf{a}_i'^*)$  the *optimal* tensors. Our theory is that, by *proper similarity transformations*, the optimal tensors in the middle part of the tensor chain can be transformed into translation-invariant tensors, i.e.,

$$T_i = T, \quad (13)$$

with  $T$  the transfer matrix. Suppose the depth of the boundary regions is  $\ell_B$ , and then the nonlocality measure permitted by the transfer-matrix theory is expressed as

$$\mathcal{S}_n^{(\ell_B)} = \max_{\bar{\mathbf{a}}} \langle T_1 | T_2 \cdots T_{\ell_B} T^{n-2\ell_B} T_{n-\ell_B+1} \cdots T_{n-1} | T_n \rangle, \quad (14)$$

where  $\bar{\mathbf{a}}$  is a set of  $2(2\ell_B + 1)$  (rather than  $2n$ ) unit vectors. Please see Fig. 2(c).  $\ell_B$  controls the accuracy of the transfer-matrix theory. For instance, when  $\ell_B \rightarrow \frac{n}{2}$ , the translation-invariant regions vanish, thus  $\mathcal{S}_n^{(\ell_B)}$  should fully reproduce Eq. (12). Nevertheless, as we will show by several models, even when  $\ell_B$  is quite small (i.e.,  $\ell_B \ll n$ ),  $\mathcal{S}_n^{(\ell_B)}$  can reproduce Eq. (12).

#### IV. NUMERICAL RESULTS AND APPLICATIONS

*Model 1:  $J_1$ - $J_2$ - $\alpha$  model.* As the first example, we will consider a bond-alternating spin- $\frac{1}{2}$  Heisenberg chain with next-nearest-neighbor interactions [36,37],

$$\hat{H} = J_1 \sum_{\text{odd } i} \mathbf{S}_i \cdot \mathbf{S}_{i+1} + J_2 \sum_{\text{even } i} \mathbf{S}_i \cdot \mathbf{S}_{i+1} + \alpha \sum_i \mathbf{S}_i \cdot \mathbf{S}_{i+2}. \quad (15)$$

$J_1$  and  $J_2$  denote bond-alternating couplings, and  $\alpha$  denotes next-nearest-neighbor coupling.

In the parameter space  $-2\alpha + \frac{J_2 - J_1}{2} = -1$  [38], it is well known that the ground state  $|\psi\rangle$  is a singlet-product state, which can be described by an infinite-size MPS consisting of two-qubit unit cells, i.e.,  $A_0 = (0, -1)$ ,  $A_1 = (1, 0)$ ,  $B_0 = (\sqrt{2}, 0)$ , and  $B_1 = (\sqrt{2}, 0)$ . We have optimized Eq. (12) numerically and find that  $\mathcal{S}_n = \sqrt{2}$ , i.e., an  $n$ -independent constant. This result can be perfectly reproduced by optimizing Eq. (14). In fact, even just with  $\ell_B = 1$ , the optimal solution gives  $T_1 = (\sqrt{2}, 0)$ ,  $T_n = (\sqrt{2}, 0)$ , and  $T_i = \begin{pmatrix} 1 & 0 \\ 0 & 1 \end{pmatrix}$  for  $1 < i < n$ . Thus Eq. (12) is reproduced by the transfer-matrix theory with  $\ell_B = 1$ .

*Model 2: Transverse-field Ising model.* We consider the 1D transverse-field Ising chain described by

$$\hat{H} = - \sum_i \hat{\sigma}_z^i \hat{\sigma}_z^{i+1} - h \sum_i \hat{\sigma}_x^i, \quad (16)$$

where  $\hat{\sigma}_{x,z}^i$  are Pauli matrices on qubit  $i$ , and  $h$  denotes the strength of the magnetic field along the  $x$  direction.  $h = 1$  is a quantum critical point. We have used an infinite time-evolving block decimation algorithm [39,40] (with  $D \leq 8$ ) and the Matrix-Product Toolkit [41] (with  $D \geq 10$ ) to express the ground states of the chains into MPSs [31].

We find the transfer-matrix theory in Eq. (14) with  $\ell_B = 1$  cannot fully reproduce the best results of Eq. (12) anymore. Thereby, we carry out the optimizations of Eq. (14) with  $\ell_B$  increasing step by step, and the results (with  $n = 40$ ) are shown in Fig. 3. As  $\ell_B$  increases,  $\log_2 \mathcal{S}_n^{(\ell_B)}$  converges rather fast.

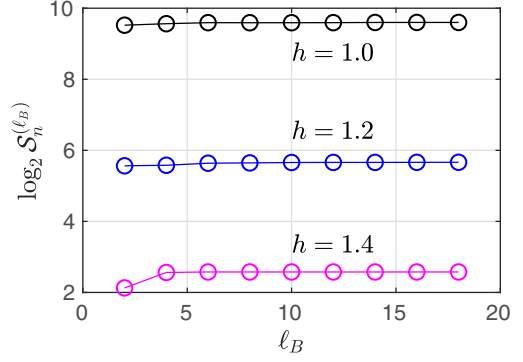


FIG. 3. Logarithm nonlocality measure from the transfer-matrix theory as a function of the boundary depth  $\ell_B$ . The transverse-field Ising model is used as an example, with  $h$  the strength of the magnetic field. The bond dimension of the MPS is  $D = 8$ . The length of the subchain is  $n = 40$ . As  $\ell_B$  increases,  $\log_2 \mathcal{S}_n^{(\ell_B)}$  converges rather fast. It indicates that the transfer-matrix theory in Fig. 2(c) with quite small  $\ell_B$  is sufficient to reproduce the best results of Fig. 2(b).

For instance, for  $h = 1.4$ , we find  $\log_2 \mathcal{S}_n^{(\ell_B)} = 2.5761$  when  $\ell_B = 6$ . On the other hand, Eq. (12) gives  $\log_2 \mathcal{S}_n = 2.5762$ . Thereby, the results of  $\mathcal{S}_n$  in the transverse-field Ising model are also reproduced by the transfer matrix theory  $\mathcal{S}_n^{(\ell_B)}$  with  $\ell_B \ll n$ .

*Scaling and its origin.* The scaling behaviors of  $\mathcal{S}_n$  can be explained uniformly by the transfer-matrix theory. We denote the eigenvalues of the transfer matrix  $T$  as  $\lambda_i$ . Then according to Eq. (14), it is easy to prove that only  $\lambda_{\max}$ —the eigenvalue with the largest magnitude—would play a role in the large- $n$  limit, i.e.,

$$\mathcal{S}_n^{(\ell_B)} \xrightarrow{n \rightarrow \infty} |\lambda_{\max}|^{n-2\ell_B} p, \quad (17)$$

with  $p$  an  $n$ -independent quantity.  $|\cdot|$  denotes the absolute value when  $\lambda_i$  are real and denotes the complex modulus when  $\lambda_i$  are complex.

If  $|\lambda_{\max}| < 1$ ,  $\mathcal{S}_n^{(\ell_B)}$  would vanish in the large- $n$  limit. If  $|\lambda_{\max}| = 1$  (such as in the  $J_1$ - $J_2$ - $\alpha$  model, where the transfer matrix is just the identity matrix),  $\mathcal{S}_n^{(\ell_B)}$  would be an  $n$ -independent constant. If  $|\lambda_{\max}| > 1$ , however, we have

$$\log_2 \mathcal{S}_n^{(\ell_B)} = n \log_2 |\lambda_{\max}| + \log_2 \frac{p}{|\lambda_{\max}|^{2\ell_B}}, \quad (18)$$

where

$$\mathcal{K} := \log_2 |\lambda_{\max}| \quad (19)$$

is just the central parameter in the scaling formula.

The theory can be generalized to quantum systems with large unit cells. For instance, for ground states which consist of two-qubit unit cells, we use two qubits to define the transfer matrix, i.e.,  $T = T_i T_{i+1}$ , and then  $\mathcal{K}$  should be given by

$$\mathcal{K} = \log_2 |\lambda_{\max}|^{\frac{1}{2}}. \quad (20)$$

Finally, the scaling behaviors observed in various 1D quantum lattices in previous papers are explained uniformly by the transfer-matrix theory.

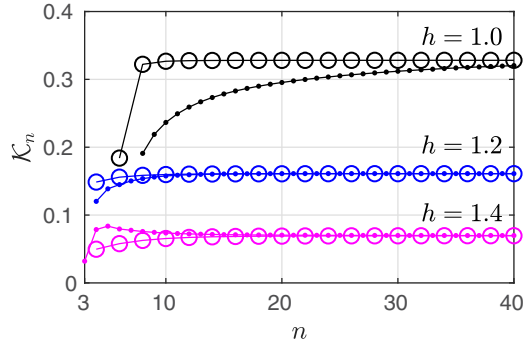


FIG. 4. Central parameter  $\mathcal{K} = \lim_{n \rightarrow \infty} \mathcal{K}_n$  of the transverse-field Ising model. The bond dimension of the MPS is  $D = 8$ . Circles denote the results from the transfer-matrix theory combined with an  $n$ -qubit optimization algorithm. Dots denote the results from a traditional approach [31] for a comparison purpose. At the critical point  $h = 1.0$ , the transfer-matrix approach converges much faster than the traditional approach.

The origin of the scaling behaviors of  $\mathcal{S}_n$  is quite clear. For 1D quantum chains which are translation invariant, the optimal nonlocality operators also present some hidden translation invariance, captured by the transfer-matrix theory.

*Application:* Fast-convergence algorithms for calculating  $\mathcal{K}$ . For finite-size lattices  $\mathcal{S}_n$  is a meaningful measure of multipartite correlations. For infinite-size lattices with  $n \rightarrow \infty$ , however,  $\log_2 \mathcal{S}_n \sim \mathcal{K}n + b$  diverges in most situations. Then, the central parameter  $\mathcal{K}$  provides us a valuable tool to characterize multipartite correlations in infinite-size systems.  $\mathcal{K}$  has a clear physical meaning. According to Eq. (2), it is not difficult to find that  $\mathcal{K} \leq \frac{1}{2}$ , and  $\mathcal{K} \rightarrow \frac{1}{2}$  indicates high hierarchy of multipartite nonlocality. On the other hand, for the lowest hierarchy of multipartite nonlocality, we have  $\mathcal{K} \rightarrow 0$ . Thereby,  $\mathcal{K}$  can characterize the hierarchy of multipartite nonlocality in infinite-size systems.

In a traditional approach to calculate  $\mathcal{K}$ , one calculates the derivative  $\mathcal{K}_n = \frac{\partial \log_2 \mathcal{S}_n}{\partial n}$  of the  $\log_2 \mathcal{S}_n \sim n$  curve and takes the large- $n$  limit, i.e.,  $\mathcal{K} = \lim_{n \rightarrow \infty} \mathcal{K}_n$  [31]. A drawback of this approach is that  $\mathcal{K}_n$  converges slowly in the critical regions (see the solid dots in Fig. 4).

According to the transfer-matrix theory, the central parameter  $\mathcal{K}$  is determined just by the largest-magnitude eigenvalue of the transfer matrix. Therefore, for an  $n$ -qubit lattice, suppose we have already figured out an optimal solution  $\bar{\mathbf{a}}^*$ . Then we can move on to construct the transfer matrix by the tensors in the middle of the chain, i.e.,  $T = T_{\frac{n}{2}} T_{\frac{n}{2}+1}$ . Then the finite-size parameter  $\mathcal{K}_n$  would be given by  $\mathcal{K}_n = \log_2 |\lambda_{\max}|^{\frac{1}{2}}$ . We will increase  $n$  until some convergence is obtained. The advantage of this approach is that the contributions of other eigenvalues  $|\lambda_i| < |\lambda_{\max}|$ , which play no role in the large- $n$  limit [see Eq. (17)], are eliminated from the beginning.

Our numerical results for the transverse-field Ising model are illustrated in Fig. 4. In the noncritical regions (i.e.,  $h = 1.2$  and  $h = 1.4$ ), the traditional approach (dots) and the transfer-matrix approach (circles) converge fast to an equal value; thus the validity of the transfer-matrix approach is

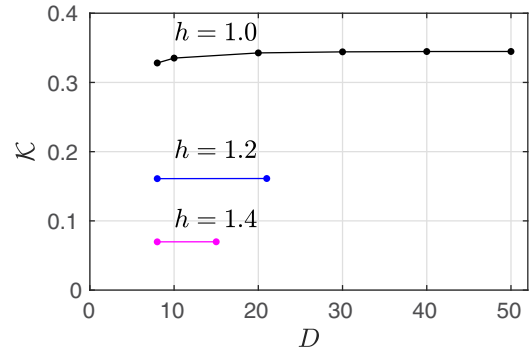


FIG. 5.  $D$  dependence of the central parameter  $\mathcal{K}$  in the transverse-field Ising model. For  $D = 8$ , the results are from the converged results in Fig. 4. For  $D \geq 10$ , the ground states are calculated using the Matrix-Product Toolkit [41] and  $\mathcal{K}$  is calculated with the second transfer-matrix algorithm.

confirmed. For the critical field  $h = 1.0$ , however, the traditional approach converges rather slowly (i.e.,  $\mathcal{K}_{24} = 0.3035 < \mathcal{K}_{40} = 0.3203$ ), while the transfer-matrix approach converges quite fast (i.e.,  $\mathcal{K}_{24} = \mathcal{K}_{40} = 0.3281$ ). Thereby, this transfer-matrix approach greatly improves the speed of convergence of  $\mathcal{K}$  in the quantum critical regions. This algorithm will be called our first algorithm, in which the transfer-matrix theory is combined with an  $n$ -qubit optimization algorithm for calculating  $\mathcal{S}_n$ .

Here we recommend a second algorithm to directly calculate  $\mathcal{K}$  that is even more strategic and efficient. For brevity, we consider a single-site transfer matrix  $T$  as

$$T(\mathbf{a}, \mathbf{a}') = \sum_{ss'} A_s \otimes [\sigma(\mathbf{a}, \mathbf{a}')]_{ss'} \otimes A_{s'}^*. \quad (21)$$

Our goal is to optimize the largest-magnitude eigenvalue  $|\lambda_{\max}|$  of this transfer matrix with respect to the unit vectors  $\{\mathbf{a}, \mathbf{a}'\}$ . When this optimization is finished, the central parameter  $\mathcal{K}$  is simply given by Eq. (19). We have used this algorithm to recalculate the transverse-field Ising model. For  $h = 1, 1.2$ , and  $1.4$ , the central parameter  $\mathcal{K}$  turns out to be  $0.3281, 0.1610$ , and  $0.0697$ , respectively. As a comparison, we mention that values of  $\mathcal{K}_{40}$  in Fig. 4 are  $0.3281, 0.1610$ , and  $0.06955$ , respectively. Thereby the validity of this second algorithm is confirmed.

This powerful algorithm deserves some further comments. First of all, compared with the first algorithm, the  $n$ -qubit optimization of the measure  $\mathcal{S}_n$  is completely avoided, and thus the code becomes much more simple. Second, since it directly calculates  $\mathcal{K}$ , there is no  $n$ -related convergence problem that appears in the first algorithm (see Fig. 4). Third, in this algorithm, the most time-consuming step is to figure out the eigenvalue of the  $2D^2 \times 2D^2$  transfer matrix  $T$  for hundreds of rounds. When  $D$  is not too large (which is just the situation in the Ising model), we find the computational efficiency is significantly better than in the first algorithm. Thereby, we are able to analyze the  $D$  dependence of  $\mathcal{K}$  (see Fig. 5). When  $D$  is very large, however, the diagonalization of the matrix  $T$  would become computationally intensive.

## V. SUMMARY AND SOME PERSPECTIVES

In this paper, we have proposed a transfer-matrix theory to reveal the hidden translation invariance in the optimal nonlocality operators in 1D quantum lattices, and verified the theory numerically by considering several typical quantum models. The theory discloses that the scaling of the nonlocality measure  $\mathcal{S}_n$  is determined by the largest-magnitude eigenvalue  $\lambda_{\max}$  of the transfer matrix, i.e.,  $\mathcal{S}_n \sim |\lambda_{\max}|^n$ , and thus offers a unified explanation for previously observed scaling behaviors in various 1D quantum lattices. Another result of this paper is that the central parameter  $\mathcal{K}$ , which characterizes multipartite nonlocality for 1D infinite-size quantum chains, is determined by the optimal transfer matrix as  $\mathcal{K} = \log_2 |\lambda_{\max}|$ . Thereby, powerful transfer-matrix-based algorithms are proposed to calculate  $\mathcal{K}$ . We have shown unambiguously that in quantum critical regions, the transfer-matrix algorithms present a much faster convergence speed than the traditional approach.

Mere ground states have been considered in this paper. At finite temperatures, the thermal states of 1D quantum lattices can also be expressed by translation-invariant tensor networks [42]. Thereby, we believe the transfer-matrix theory can also be applied to finite temperatures and will be investigated in our future work. Moreover, the theory offers a clue to design feasible Bell-type experiments in solid materials.

## ACKNOWLEDGMENTS

We would like to express our great gratitude to the anonymous referees of this paper. The algorithm to directly optimize the largest-magnitude eigenvalue of the transfer matrix is proposed by one of the referees. We would like to thank Professor Ian McCulloch for his great software Matrix-Product Toolkit. The research was supported by the National Natural Science Foundation of China (Grant No. 11675124).

## APPENDIX: ORDERINGS OF THE QUBITS

In the construction of the nonlocality operator  $\hat{M}_n$  in Eq. (1), the specific ordering  $(n, n-1, n-2, \dots, 1)$  of the qubits has been used. One may ask what will happen if we use other orderings to construct  $\hat{M}_n$ . Consider the expression

$$\mathcal{S}_n = \max_{\bar{a}} \text{tr}[\hat{\rho}_n \hat{M}_n(\bar{a})]. \quad (\text{A1})$$

When some other ordering is used, one keeps  $\hat{\rho}_n$  unchanged and transforms  $\hat{M}_n$  into  $\hat{M}'_n = \hat{P} \hat{M}_n \hat{P}^{-1}$ , where  $\hat{P}$  is the permuting operator associated with the concerned new ordering. Or alternatively, one may keep  $\hat{M}_n$  unchanged and transform the origin state  $\hat{\rho}_n$  into  $\hat{P} \hat{\rho}_n \hat{P}^{-1}$ . We use the latter approach. So, the question becomes, for arbitrary permuting operator  $\hat{P}$ , are  $\mathcal{S}_n(\hat{\rho}_n)$  and  $\mathcal{S}_n(\hat{P} \hat{\rho}_n \hat{P}^{-1})$  equal to each other? If the answer is yes, then the orderings of the qubits can be ignored in our study. If the answer is no, then some multipartite nonlocal correlations may be missed when other orderings are not considered.

First, let us investigate the simplest situation, i.e., two-qubit states. There are only two orderings, i.e., (2,1) and (1,2), where the corresponding states will be marked as  $\hat{\rho}_{(2,1)}$  and  $\hat{\rho}_{(1,2)}$ , respectively. Our conclusion is that  $\mathcal{S}_2(\hat{\rho}_{(2,1)}) =$

$\mathcal{S}_2(\hat{\rho}_{(1,2)})$ . According to Horodecki *et al.*'s work, an analytical expression for  $\mathcal{S}_2$  exists for general two-qubit states [43]. For  $\hat{\rho}_{(2,1)}$ , a  $3 \times 3$  matrix  $\Lambda$  is defined as

$$\Lambda_{ij} = \text{tr}(\hat{\rho}_{(2,1)} \hat{\sigma}_i \otimes \hat{\sigma}_j) \quad (\text{A2})$$

with  $i, j = \{x, y, z\}$ . Then Horodecki *et al.* have proved that  $\mathcal{S}_2(\hat{\rho}_{(2,1)}) = \sqrt{\lambda_1 + \lambda_2}$ , with  $\lambda_1$  and  $\lambda_2$  the two largest eigenvalues for the symmetric matrix  $\Lambda^T \Lambda$ . Here the superscript  $T$  represents the transpose of the matrix.

For  $\hat{\rho}_{(1,2)} = \hat{P} \hat{\rho}_{(2,1)} \hat{P}^{-1}$ , the elements of the  $3 \times 3$  matrix become

$$\tilde{\Lambda}_{ij} = \text{tr}(\hat{P} \hat{\rho}_{(2,1)} \hat{P}^{-1} \hat{\sigma}_i \otimes \hat{\sigma}_j) = \text{tr}(\hat{\rho}_{(2,1)} \hat{\sigma}_j \otimes \hat{\sigma}_i) = \Lambda_{ji}. \quad (\text{A3})$$

Then we have  $\mathcal{S}_2(\hat{\rho}_{(1,2)}) = \sqrt{\tilde{\lambda}_1 + \tilde{\lambda}_2}$  with  $\tilde{\lambda}_1$  and  $\tilde{\lambda}_2$  the two largest eigenvalues of  $\tilde{\Lambda}^T \tilde{\Lambda}$ . In Eq. (A3), it is clear that  $\tilde{\Lambda} = \Lambda^T$ . Thus,  $\tilde{\Lambda}^T \tilde{\Lambda}$  and  $\Lambda^T \Lambda$  would have the same eigenvalues. Therefore, for arbitrary two-qubit state we always have

$$\mathcal{S}_2(\hat{\rho}_{(2,1)}) = \mathcal{S}_2(\hat{\rho}_{(1,2)}). \quad (\text{A4})$$

For  $n > 2$ , no analytical expression for  $\mathcal{S}_n$  exists. Thereby, we have to consider all the possible orderings numerically.

For  $n = 3$ , one can see that there are a total of six orderings, i.e., (3,2,1), (3,1,2), (2,3,1), (2,1,3), (1,3,2), and (1,2,3). We have considered the ground state of the three-qubit transverse-field Ising model in Eq. (16) with  $h = 1$ . We have figured out all six permuted density matrices  $\hat{\rho}_{(3,2,1)}$ ,  $\hat{\rho}_{(3,1,2)}$ ,  $\hat{\rho}_{(2,3,1)}$ , and so on. For each of these six density matrices, we have carried out the numerical optimization  $\max_{\bar{a}} \text{tr}(\hat{\rho} \hat{M}_n)$  independently, and they all lead to the same result, i.e.,

$$\mathcal{S}_3(\hat{\rho}_{(3,2,1)}) = \mathcal{S}_3(\hat{\rho}_{(3,1,2)}) = \mathcal{S}_3(\hat{\rho}_{(2,3,1)}) = \dots = 1.2471. \quad (\text{A5})$$

As a second example, we have initialized a random three-qubit quantum state. Again, the nonlocality measures for the permuted density matrices are equal to each other, i.e.,

$$\mathcal{S}_3(\hat{\rho}_{(3,2,1)}) = \mathcal{S}_3(\hat{\rho}_{(3,1,2)}) = \mathcal{S}_3(\hat{\rho}_{(2,3,1)}) = \dots \quad (\text{A6})$$

For  $n = 4$ , there are a total of 24 orderings, i.e., (4,3,2,1), (4,3,1,2), (4,2,3,1), (4,2,1,3), and so on. We have considered the ground state of the four-qubit transverse-field Ising model with  $h = 1$ , and have figured out all 24 permuted density matrices. It turns out that they all lead to the same result, i.e.,

$$\mathcal{S}_4(\hat{\rho}_{(4,3,2,1)}) = \mathcal{S}_4(\hat{\rho}_{(4,3,1,2)}) = \mathcal{S}_4(\hat{\rho}_{(4,2,3,1)}) = \dots = 1.4328. \quad (\text{A7})$$

We have also initialized a random four-qubit quantum state, and figured out all 24 permuted density matrices. Again, all these density matrices lead to the same value of  $\mathcal{S}_4$ , i.e.,

$$\mathcal{S}_4(\hat{\rho}_{(4,3,2,1)}) = \mathcal{S}_4(\hat{\rho}_{(4,3,1,2)}) = \mathcal{S}_4(\hat{\rho}_{(4,2,3,1)}) = \dots \quad (\text{A8})$$

We mention that in the random quantum states, symmetries (such as the translation invariance and the permutation invariance) are not present.

Our analytical result for general two-qubit states and numerical results for three-qubit and four-qubit states suggest that the permutation operators do not change the value of the nonlocality measure  $\mathcal{S}_n$ . [For a fixed  $\bar{a}$ , the permutation operator  $\hat{P}$  changes the value of  $\text{tr}[\hat{\rho}_n \hat{M}_n(\bar{a})]$  if the state

does not have a permutation invariance. Nevertheless, our results show that  $\hat{P}$  does not change the optimization result  $\max_{\vec{a}} \text{tr}[\hat{\rho}_n \hat{M}_n(\vec{a})]$ , in other words, the nonlocality measure  $\mathcal{S}_n$ .] Thereby, when using the Mermin-Klyshko-Bell inequal-

ities to analyze multipartite nonlocality in general  $n$ -qubit states, we believe the orderings of the qubits do not play an important role. It may be interesting to find a rigorous proof in our future work.

- 
- [1] J. Eisert, M. Cramer, and M. B. Plenio, *Rev. Mod. Phys.* **82**, 277 (2010).
- [2] U. Schollwöck, *Ann. Phys.* **326**, 96 (2011).
- [3] O. Gühne, G. Tóth, and H. J. Briegel, *New J. Phys.* **7**, 229 (2005).
- [4] F. Levi and F. Mintert, *Phys. Rev. Lett.* **110**, 150402 (2013).
- [5] K. Kato, F. Furrer, and M. Murao, *Phys. Rev. A* **93**, 022317 (2016).
- [6] C. Radhakrishnan, M. Laurière, and T. Byrnes, *Phys. Rev. Lett.* **124**, 110401 (2020).
- [7] Z. Ren, W. Li, A. Smerzi, and M. Gessner, *Phys. Rev. Lett.* **126**, 080502 (2021).
- [8] S. Nezami and M. Walter, *Phys. Rev. Lett.* **125**, 241602 (2020).
- [9] M. Brenes, S. Pappalardi, J. Goold, and A. Silva, *Phys. Rev. Lett.* **124**, 040605 (2020).
- [10] C. Harney, S. Pirandola, A. Ferraro, and M. Paternostro, *New J. Phys.* **22**, 045001 (2020).
- [11] M. Navascués, E. Wolfe, D. Rosset, and A. Pozas-Kerstjens, *Phys. Rev. Lett.* **125**, 240505 (2020).
- [12] D. Collins, N. Gisin, S. Popescu, D. Roberts, and V. Scarani, *Phys. Rev. Lett.* **88**, 170405 (2002).
- [13] D. Collins, N. Gisin, N. Linden, S. Massar, and S. Popescu, *Phys. Rev. Lett.* **88**, 040404 (2002).
- [14] Q. Y. He, E. G. Cavalcanti, M. D. Reid, and P. D. Drummond, *Phys. Rev. Lett.* **103**, 180402 (2009).
- [15] J.-D. Bancal, C. Branciard, N. Gisin, and S. Pironio, *Phys. Rev. Lett.* **103**, 090503 (2009).
- [16] J.-D. Bancal, N. Brunner, N. Gisin, and Y.-C. Liang, *Phys. Rev. Lett.* **106**, 020405 (2011).
- [17] N. Brunner, J. Sharam, and T. Vértesi, *Phys. Rev. Lett.* **108**, 110501 (2012).
- [18] I. Šupić, J.-D. Bancal, and N. Brunner, *Phys. Rev. Lett.* **125**, 240403 (2020).
- [19] P. Contreras-Tejada, C. Palazuelos, and J. I. de Vicente, *Phys. Rev. Lett.* **126**, 040501 (2021).
- [20] Z.-Y. Sun, Y.-Y. Wu, J. Xu, H.-L. Huang, B.-F. Zhan, B. Wang, and C.-B. Duan, *Phys. Rev. A* **89**, 022101 (2014).
- [21] S. Campbell and M. Paternostro, *Phys. Rev. A* **82**, 042324 (2010).
- [22] Z.-Y. Sun, M. Wang, Y.-Y. Wu, and B. Guo, *Phys. Rev. A* **99**, 042323 (2019).
- [23] L. Justino and T. R. de Oliveira, *Phys. Rev. A* **85**, 052128 (2012).
- [24] Z.-Y. Sun, S. Liu, H.-L. Huang, D. Zhang, Y.-Y. Wu, J. Xu, B.-F. Zhan, H.-G. Cheng, C.-B. Duan, and B. Wang, *Phys. Rev. A* **90**, 062129 (2014).
- [25] Y. Dai, C. Zhang, W. You, Y. Dong, and C. H. Oh, *Phys. Rev. A* **96**, 012336 (2017).
- [26] H.-G. Cheng, M. Li, Y.-Y. Wu, M. Wang, D. Zhang, J. Bao, B. Guo, and Z.-Y. Sun, *Phys. Rev. A* **101**, 052116 (2020).
- [27] Z.-Y. Sun, X. Guo, and M. Wang, *Eur. Phys. J. B* **92**, 75 (2019).
- [28] J. Bao, B. Guo, H.-G. Cheng, M. Zhou, J. Fu, Y.-C. Deng, and Z.-Y. Sun, *Phys. Rev. A* **101**, 012110 (2020).
- [29] D.-L. Deng, C. Wu, J.-L. Chen, S.-J. Gu, S. Yu, and C. H. Oh, *Phys. Rev. A* **86**, 032305 (2012).
- [30] S. Sachdev, *Quantum Phase Transitions* (Cambridge University Press, Cambridge, U.K., 1999).
- [31] Z.-Y. Sun, B. Guo, and H.-L. Huang, *Phys. Rev. A* **92**, 022120 (2015).
- [32] N. D. Mermin, *Phys. Rev. Lett.* **65**, 1838 (1990).
- [33] A. V. Belinski and D. N. Klyshko, *Phys. Usp.* **36**, 653 (1993).
- [34] V. Scarani and N. Gisin, *J. Phys. A: Math. Gen.* **34**, 6043 (2001).
- [35] Z.-Y. Sun, M. Li, L.-H. Sheng, and B. Guo, *Phys. Rev. A* **103**, 052205 (2021).
- [36] H. T. Wang, B. Li, and S. Y. Cho, *Phys. Rev. B* **87**, 054402 (2013).
- [37] G.-H. Liu, W.-L. You, W. Li, and G. Su, *J. Phys.: Condens. Matter* **27**, 165602 (2015).
- [38] B. S. Shastri and B. Sutherland, *Phys. Rev. Lett.* **47**, 964 (1981).
- [39] G. Vidal, *Phys. Rev. Lett.* **91**, 147902 (2003).
- [40] B. Pirvu, V. Murg, J. I. Cirac, and F. Verstraete, *New J. Phys.* **12**, 025012 (2010).
- [41] I. P. McCulloch and M. Gulácsi, *Europhys. Lett.* **57**, 852 (2002).
- [42] F. Verstraete, J. J. García-Ripoll, and J. I. Cirac, *Phys. Rev. Lett.* **93**, 207204 (2004).
- [43] R. Horodecki, P. Horodecki, and M. Horodecki, *Phys. Lett. A* **200**, 340 (1995).